Multifractal Analysis of Heliospheric Magnetic Field Fluctuations Observed by *Ulysses*

Anna Wawrzaszek[1] , Marius Echim[2,3] , and Roberto Bruno[4]
[1] Space Research Centre, Polish Academy of Sciences Bartycka 18 A 00-716 Warsaw, Poland; anna.wawrzaszek@cbk.waw.pl
[2] Royal Belgian Institute for Space Aeronomy, Brussels, Belgium; marius.echim@oma.be
[3] Institute of Space Science, Măgurele, Romania
[4] Institute for Space Astrophysics and Planetology, Roma, Italy; roberto.bruno@inaf.it

Abstract

We present the multifractal study of the intermittency of the magnetic field turbulence in the fast and slow solar wind beyond the ecliptic plane during two solar minima (1997–1998, 2007–2008) and solar maximum (1999–2001). More precisely, we consider 126 time intervals of *Ulysses* magnetic field measurements, obtain the multifractal spectra, and examine the degree of multifractality as the measure of intermittency in the MHD range of scales, for a wide range of heliocentric distances and heliolatitudes. The results show a slow decrease of intermittency with the radial distance, which is more significant for the fast than for the slow solar wind. Analysis of Alfvénic and compressive fluctuations confirms the decrease of intermittency with distance and latitude. This radial dependence of multifractality/intermittency may be explained by a slower evolution of turbulence beyond the ecliptic plane and by the reduced efficiency of intermittency drivers with the distance from the Sun. Additionally, our analysis shows that the greatest differences between magnetic field components are revealed close to the Sun, where intermittency is the strongest. Moreover, we observe that the slow solar wind from the maximum of the solar cycle 23 exhibits in general, a lower level of multifractality (intermittency) than fast solar wind, which can be related to the idea of a new type of Alfvénic slow solar wind.

Key words: interplanetary medium – magnetic fields – solar wind – turbulence

1. Introduction

Turbulence in the solar wind was analyzed extensively based on measurements acquired from various space missions (see Bruno & Carbone 2013 for review). A large number of studies focused on the existence of the intermittency and its role for the inertial range turbulence (e.g., Burlaga 1991a; Marsch & Liu 1993; Tu et al. 1996; Sorriso-Valvo et al. 1999; Bruno et al. 2003), as well as for processes in the kinetic range (Perri et al. 2012; Wan et al. 2012; Sorriso-Valvo et al. 2017). Intermittency was analyzed from the anomalous scaling of structure functions (e.g., Burlaga 1991a, 1995; Marsch & Liu 1993; Horbury et al. 1997), from the non-Gaussian behavior of probability distribution functions (PDFs) of the solar wind fluctuation (Marsch & Tu 1994), by using Castaing distributions (Castaing et al. 1990; Sorriso-Valvo et al. 1999, 2001; Pagel & Balogh 2003) or the fourth moment (kurtosis) as a first indicator of intermittency (e.g., Bruno et al. 2003; Yordanova et al. 2009). Some authors quantified the intermittency from the local intermittency measure based on wavelet analysis (Farge 1992; Veltri & Mangeney 1999; Bruno et al. 2001) or from the multifractal description (e.g., Marsch et al. 1996; Burlaga & Ness 2010; Wawrzaszek & Macek 2010; Wawrzaszek et al. 2015). In general, the analysis showed that intermittency is a real characteristic of turbulence in the slow and fast solar wind, during solar minimum and solar maximum, in the inner and outer heliosphere (see, e.g., Burlaga 1991a, 1991b; Marsch & Liu 1993), further in the heliosheath (Burlaga & Ness 2010; Macek et al. 2011), and even near the heliopause (Macek et al. 2014).

In particular, Marsch & Liu (1993) showed that small scales are more intermittent than large scales, the fast solar wind is generally less intermittent than slow wind. Moreover, the radial component of the fluctuations in the fast solar wind is more intermittent than the transverse components. A comparison between fast and slow streams at two heliocentric distances, namely at 0.3 and 1 au, allowed authors to suggest also the radial evolution of intermittency in the ecliptic.

Tu et al. (1996) using *Helios* data (3 cases from slow and 2 from fast solar wind) studied the intermittent nature of magnetic field fluctuations in the range of scales 81–2500 s. They examined the structure function scaling and showed that while the intermittency in the fast solar wind is relatively stable, the intermittency parameter for the magnetic components in the slow wind varies significantly, from relatively low values to very high ones, but without the clear radial evolution trend.

Sorriso-Valvo et al. (1999) used the Castaing distribution to analyze the fluctuation observed by *Helios* 2 at timescales from 81 s to 1 day and showed that the magnetic field strength is more intermittent than bulk speed in the fast and slow streams. Moreover, they indicated that the intermittency of the magnetic field intensity was roughly the same for both slow and fast wind.

Bruno et al. (2003) analyzed the flatness of magnetic field and velocity PDF at 0.3, 0.7, and 0.9 au and concluded that intermittency in the fast solar wind increases with the increase of the distance from the Sun, while slow wind intermittency does not show radial dependence. They also considered the intermittency of the components rotated into the mean field reference system and showed that the most intermittent magnetic component is the one along the mean field, while the perpendicular ones show a similar level of intermittency within the associated uncertainties. Moreover, when the radial distance increases, the component along the mean field becomes more and more intermittent compared to the transverse ones.

These results were obtained from the ecliptic plane data, where velocity shear, parametric decay, and interaction of

Alfvénic modes with convected structures plays an important role (Bruno & Carbone 2013). Beyond the ecliptic plane, the state of turbulence differs from that observed in the equatorial region (Ruzmaikin et al. 1995; Bavassano et al. 2000, 2001). Various studies showed that the evolution of turbulence in the polar wind is less rapid (e.g., Horbury et al. 1996; Bruno & Trenchi 2014). The state of the turbulence influences the intermittency level, as shown for interplanetary magnetic field fluctuations (e.g., Ruzmaikin et al. 1995; Horbury & Balogh 2001; Pagel & Balogh 2002, 2003; Yordanova et al. 2009).

In particular, Pagel & Balogh (2001) analyzed structure function scaling and used several intermittency models to look at small-scale magnetic field fluctuations in the solar wind measured by *Ulysses* during solar minimum (1994–1995), at radial distances 1.3 and 2.4 au (heliolatitudes varied from 80°S to 80°N). Concentrating on the range of scales between 10 and 300 s they indicated the high level of intermittency in the fast solar wind and showed how much more variable and difficult to interpret the state of the slow solar wind is. Transverse components showed a very similar level of intermittency, while the radial component values were slightly lower.

In another study, Pagel & Balogh (2002) confirmed that magnetic field components present a high level of intermittency at minimum (1994–1996) and at maximum (2000–2001) phases of the solar cycle, and showed that the slow solar wind has a lower level of intermittency compared to the fast flow. However, these authors used only the wind speed as the criterion to discriminate between pure coronal fast and typical equatorial slow wind.

Pagel & Balogh (2003) fitted the PDFs of magnetic field fluctuations with the Castaing distribution for timescales between 40 and 200 s. They analyzed 28 cases of the pure polar coronal fast wind at solar minimum, between 1994 and 1996, and showed that intermittency of the magnetic field fluctuations increased with increasing the radial distance in the range 1.4–4.1 au. The same authors showed that, in the RTN reference system, the transverse magnetic field components are significantly more non-Gaussian than the radial component.

Yordanova et al. (2009) performed a detailed selection of the four states of the solar wind (pure fast, fast streams, pure slow, and slow streams) measured by *Ulysses* during 1992–1997. In summary, the authors considered 21 time intervals of length varied from 2 to 19 days. Their analysis of flatness performed by using 20 s averages showed that only pure fast wind presents evolution with the heliocentric distance in the considered range between 1.5 and 3.0 au and at latitudes between 50° and 80°. However, it is worth stressing that this evolution has been identified on the basis of four cases only (Yordanova et al. 2009, Table 1). Yordanova et al. concluded that pure slow wind measured at 5.1–5.4 au and at latitudes narrowed to <20° presents the most intermittent state.

Wawrzaszek et al. (2015) performed multifractal analysis of fluctuations of the interplanetary magnetic field strength for two solar minima (1997–1998, 2007–2008) and one maximum (1999–2001). Their data included 98 time intervals of the slow and fast solar wind in the range of radial distances 1.4–5.4 au and a heliolatitude range between −80° and 70°. It was found, in general, that the level of intermittency decreases with distance and latitude. It is worth pointing out that during the identification of the multifractal scaling region, scales less than

16 s have also been included, which could influence the obtained results.

Comparative studies of solar wind intermittent turbulence beyond the ecliptic plane, especially at the solar minimum and the solar maximum, both for fast and slow solar winds, are limited and we aim to fill this gap in this work. We are convinced that further extensive studies of the intermittency phenomenon in the solar wind using the same methodology and timescales are still needed, especially in the context of better understanding the relation of the fluctuations' power within the inertial range with their nature of scaling below this range (Bruno et al. 2014). Therefore, we extend our previous studies by using a larger collection of magnetic field data sets (126 time intervals), which provides a good statistical significance and allows us to examine the evolution of the degree of multifractality as a measure of intermittency over a wide range of radial distances and heliographic latitudes explored by the *Ulysses* spacecraft. To avoid the problem of mixing of different states of the solar wind, a strict procedure of data selection is applied. This is the first time that the multifractal spectrum has been determined for three components of the interplanetary magnetic field in the MHD range (on scales higher than 16 s) at solar minima (1997–1998, 2007–2008) and maximum (1999–2001). Moreover, by using the multifractal description we also investigate the intermittency of the parallel and perpendicular components in the local Mean Field reference system, as was done by Bruno et al. (2003) for *Helios* 2 data in the ecliptic plane.

The procedure for data selection is described in Section 2. In Section 3 we briefly discuss the multifractal methodology used to quantify the intermittent state of considered data. Section 4 presents the results of the multifractal analysis, showing in particular the latitudinal and radial dependences of level of multifractality as a measure of intermittency. The results for all magnetic field components, independently on the used reference system, reveal a slow decrease of the level of intermittency with increasing distance from the Sun. Moreover, the slow solar wind measured during maximum of the cycle 23 presents a level of intermittency smaller than fast solar wind during the solar minimum of the same cycle. A summary is provided in Section 5.

2. Data Selection Process

In this study, we focus on the analysis of the magnetic field fluctuations measured by the *Ulysses* spacecraft in the slow and fast solar wind. We analyze data from two solar minima (1997–1998, 2007–2008) and one solar maximum (1999–2001). We discriminate between the fast and slow solar wind state based on data selection criteria constructed with five solar wind parameters: (1) the radial velocity, V_R, (2) the proton density, n_p, (3) the proton temperature T_p, parameters provided by the Solar Wind Observations Over the Poles of the Sun instrument (Bame et al. 1992), (4) the oxygen ion ratio (O^{+7}/O^{+6}) from the Solar Wind Ion Composition Spectrometer (Gloeckler et al. 1992), and (5) the magnetic compressibility factor C_B, defined as $C_B = (\langle |B|^2 \rangle - \langle |B| \rangle^2)/((\langle B_R^2 \rangle - \langle B_R \rangle^2) + (\langle B_T^2 \rangle - \langle B_T \rangle^2) + (\langle B_N^2 \rangle - \langle B_N \rangle^2))$ (Bruno & Bavassano 1991). B_R, B_T, and B_N are the magnetic field components measured by the VHM-FGM magnetometer (Balogh et al. 1992), while $|B|$ is the magnetic field strength. The five parameters listed above describe basic differences between slow and fast wind: the slow solar wind contrary to the fast wind is characterized by low speed, stronger

Table 1
The Threshold Values Applied to the Five Parameters Used to Select Slow and Fast Solar Wind Streams in Each Year of Three Periods of Solar Activity

Threshold	Solar Minimum		Solar Maximum			Solar Minimum	
	1997 4.7–5.4 au	1998 5.2–5.4 au	1999 4.2–5.2 au	2000 2.0–4.2 au	2001 1.3–2.6 au	2007 1.4–2.6 au	2008 2.0–4.1 au
V_{thr} (km s^{-1})	500	450	450	450	500	500	500
$(O^{+7}/O^{+6})_{thr}$	0.1	0.1	0.1	0.1	0.1	0.05	0.05
$C_{B\,thr}$	0.1	0.1	0.1	0.1	0.1	0.1	0.1
T_{thr} (K)	5×10^4 (d^a < 160) 4×10^4 (d $\geqslant$ 160)	4×10^4	5×10^4	5×10^4	1×10^5	8×10^4	8×10^4
n_{thr} (cm^{-3})	0.2	0.2	0.2	0.4 (d > 200) 1.2 (d $\geqslant$ 200)	1.5	1.5	0.7 (d < 200) 0.3 (d $\geqslant$ 200)
n_{thr} (cm^{-3}) (at 1 au)	5.2	5.7	4.5	4.9 (d > 200) 7.5 (d $\geqslant$ 200)	5.7	6.0	5.1 (d < 200) 4.2 (d $\geqslant$ 200)

Note.
[a] d denotes the day of the year.

magnetic compressibility, higher density, and lower proton temperature (Yordanova et al. 2009; Bruno & Carbone 2013; Lepri et al. 2013). We selected the oxygen charge states (O^{+7}/O^{+6}) as a diagnostic for the origin of different solar wind type (Zurbuchen et al. 2002; Yordanova et al. 2009; Landi et al. 2012). Landi et al. (2012) showed that the carbons ratio C^{+6}/C^{+4} can be considered as an even better indicator of solar wind type and region of origin. We also tested this parameter and found that it gives similar results as O^{+7}/O^{+6}. For each of the five parameters we defined a threshold value for the transition from slow to fast wind. The threshold values, listed in Table 1, have been determined empirically by visual inspection of 6 hr averages of each solar wind parameter.

The variation of the threshold values in Table 1 reflects the motion of *Ulysses* at different radial distances and heliolatitudes (Yordanova et al. 2009; Bruno & Carbone 2013; Lepri et al. 2013). Moreover, quantities in Table 1 also vary with the solar cycle (e.g., Kasper et al. 2012). The threshold values chosen for O^{+7}/O^{+6} at minimum (1997–1998) and maximum (1999–2001) are in full agreement with the previous study (Zurbuchen et al. 2002). However, for the solar minimum (2007–2008) we have identified thresholds $(O^{+7}/O^{+6})_{thr}$ two times smaller, which independently confirms the unusual character of the solar wind during this time interval and possibly significant changes occurring globally on the Sun (for more details, see, e.g., McComas et al. 2008; Lepri et al. 2013). In the final step of data selection we excluded time intervals corresponding to interplanetary transients like shocks and CMEs, identified by Gosling and Forsyth (see http://www.sp.ph.ic.ac.uk/Ulysses/shocklist.txt) and Gosling and Ebert (see http://swoops.lanl.gov/cme_list.html). Based on the procedure reported above we were able to select 126 time intervals, of which 88 correspond to fast solar wind (38 cases during solar maximum and 50 during minimum) and 38 time intervals to slow solar wind (28 during solar maximum and 10 during minimum). Each selected data set contained a few days long time series of the radial (R), transversal (T), and normal (N) component of the magnetic field measured in RTN system with resolution 1–2 vectors s^{-1}. In the RTN system, the R axis is along the radial direction, positive from the Sun to the s/c, the T component is perpendicular to the plane formed by the rotation axis of the Sun Ω and the radial direction ($T = \Omega \times R$),

and the N component resulting from the vector product $N = R \times T$ (Bruno & Carbone 2013). Moreover, in order to avoid the problem of cross-talking between the components and to provide a complete picture of the radial dependence, all data have been transformed to the mean field (hereafter MF) coordinate system. The description of the MF system can be found in Appendix D.2 of the review by Bruno & Carbone (2013), see also Bruno et al. (2003). In this reference system one of the components, $B_{\parallel}$, is parallel to the mean field B_0 and outwardly oriented, the $B_{\perp 2}$ is perpendicular to the plane containing B_0 and the R axis in the RTN system, while $B_{\perp 1}$ is the result of vector product $B_{\perp 1} = B_{\perp 2} \times B_0$ (here $B_{\perp 1}$ and $B_{\perp 2}$ indicate a unit vector).

3. Multifractal Analysis

The state of intermittency in the solar wind can be described by using several methods. In this work we apply a multifractal formalism (e.g., Halsey et al. 1986; Falconer 1990), in the frame of which both large and small concentrations of measure are taken into account, which seems to be the most appropriate to analyze the complex state of the small-scale intermittent turbulence. Multifractals can be described by functions and group of parameters (e.g., Grassberger & Procaccia 1983; Halsey et al. 1986; Falconer 1990; Ott 1993). One of the basic characteristics of multifractal scaling is the multifractal spectrum $f(\alpha)$, sketched in Figure 1 of the paper by Wawrzaszek & Macek (2010). As a function of a singularity strength α, $f(\alpha)$ portrays the variability in the scaling properties of the measures. The shape of $f(\alpha)$, in particular its width is used to quantitatively estimate the degree of multifractality of considered data (e.g., Ott 1993; Macek & Wawrzaszek 2009; Wawrzaszek & Macek 2010; Macek et al. 2014).

The multifractal spectrum can be determined with different methods (Grassberger & Procaccia 1983; Chhabra & Jensen 1989; Kantelhardt et al. 2002). In this study we apply the partition function (PF) technique (Halsey et al. 1986), successfully tested in many situations for space plasma turbulence (e.g., Macek & Szczepaniak 2008; Burlaga & Ness 2010; Lamy et al. 2010; Wawrzaszek et al. 2015). In the first step of the PF analysis, the multifractal measure is constructed by using the first moment of increments of

magnetic fluctuations,

$$\epsilon(x_i, l) = |B(x_i + l) - B(x_i)|, \quad (1)$$

where $i = 1, \ldots, N = 2^n$, with $n \geqslant 17$ denotes data set length as a power of 2, while B denotes one of the magnetic field components (B_R, B_T, B_N in RTN or $B_\parallel$, $B_{\perp 1}$, $B_{\perp 2}$ in MF reference system), separated from a position x_i by a distance l. It is worth pointing out that different measures can be constructed to emphasize various effects and to describe physical processes in data (Mandelbrot 1989; Burlaga 1995; Wawrzaszek & Macek 2010; Sorriso-Valvo et al. 2017). Next, we divide the signal into segments of size l and then each ith segment is associated with a probability measure defined by

$$p(x_i, l) \equiv \frac{\epsilon(x_i, l)}{\sum_{i=1}^{N} \epsilon(x_i, l)} = p_i(l). \quad (2)$$

This quantity can be interpreted as a probability that the portion of fluctuation is transferred to an eddy of size l. As usual, at a given position $x = v_{sw}t$, where v_{sw} is the average solar wind speed, the temporal scales measured in units of sampling time Δt can be interpreted as the spatial scales $l = v_{sw}\Delta t$ if the Taylor frozen-in-flow assumption (Taylor 1938) is satisfied (Howes et al. 2014; Perri et al. 2017). Next, the PF $\chi(q, l)$ for various values of scales l and moments q is defined as follows:

$$\chi(q, l) = \sum_{i=1}^{N(l)} (p_i(l))^q. \quad (3)$$

This definition allows us to take into account both large ($q > 0$) and small ($q < 0$) concentrations of measure, in contrast to a standard statistical description, where only positive moments are considered. Moreover, analyzing the PF (see Equation (3)), we can control and describe how moments q of measure (Equation (2)) scale with l. In particular, for a multifractal measure, this PF scales with the box size $l \to 0$ as:

$$\chi(q, l) \propto l^{\tau(q)}, \quad (4)$$

where $\tau(q)$ is the scaling exponent determined in the further step as the slopes of the logarithm of $\chi(q, l)$ (Equation (4)) versus $\log l$. The multifractal scaling range, where the linear regressions can be applied and $\tau(q)$ determined, is not known a priori, and it must be chosen for each case separately. We emphasize here that to locate the optimal scaling range an automatic selection procedure proposed by Saucier & Muller (1999) has been used. Previous studies showed that even very small scales from the dissipation region can present multifractal scaling (e.g., Sorriso-Valvo et al. 2017). The high frequency limit/break of the inertial range changes with the radial distance (Bruno & Trenchi 2014): is around 0.2/0.1/0.07 Hz at 1.4/3.2/5.3 au. Therefore, multifractal analysis has been limited to scales not smaller than 16 s. In the next step of analysis, the function $f(\alpha)$ is determined through a Legendre transformation $\alpha(q) = \frac{d}{dq}[\tau(q)] = \tau'(q)$, $f(\alpha(q)) = q\alpha(q) - \tau(q)$ (Halsey et al. 1986; Chhabra & Jensen 1989). The multifractal spectrum (α, $f(\alpha)$) is compared with the results of an independent methodology proposed by Chhabra & Jensen (1989), in which α and $f(\alpha)$ can be obtained directly from the slopes of generalized measures (e.g., Macek & Wawrzaszek 2009; Wawrzaszek & Macek 2010;

Wawrzaszek et al. 2015). Finally, the width of the singularity spectrum determined by the difference

$$\Delta \equiv \alpha_{max} - \alpha_{min}, \quad (5)$$

where $f(\alpha_{min}) = f(\alpha_{max}) = 0$, quantifies the degree of multifractality of considered data (e.g., Macek & Szczepaniak 2008). In general, the parameter Δ describes the level of inhomogeneity and is naturally related to the deviation from a strict self-similarity. That is why Δ is also a measure of intermittency, which is in contrast to self-similarity (Frisch 1995, chapter 8). In practice, owing to the limited data set, only values close to the maximum of the function $f(\alpha)$ can be calculated. Therefore, in the final step of analysis, the values α_{max} and α_{min} are fitted with a p-model for symmetric distributions (Meneveau & Sreenivasan 1987) and a two-scale binomial multiplicative cascade model for asymmetric spectra (Macek & Szczepaniak 2008). This approach was successfully used in many studies of space plasma turbulence (Burlaga et al. 1993; Macek & Szczepaniak 2008; Szczepaniak & Macek 2008; Macek & Wawrzaszek 2009; Burlaga & Ness 2010; Lamy et al. 2010). In our previous work (Wawrzaszek et al. 2015, Figure 1), we show an example of such a fit. It is worth underlining that the compatibility of the spectrum $f(\alpha)$ with the phenomenological intermittent multiplicative models confirms that multifractality at small scales is the result of intermittent nonhomogeneous cascades. Moreover, the asymmetry of the multifractal spectra can be used as an additional parameter for describing the intermittent nature of the fluctuations in the solar wind (e.g., Macek et al. 2011, 2014).

4. Results

The procedure presented above was applied to compute the multifractal spectra $f(\alpha)$ for 126 time intervals selected during two solar minima (1997–1998, 2007–2008) and one maximum (1999–2001). Next, we performed a quantitative analysis on how the widths of these spectra $f(\alpha)$ change; we determined the degree of multifractality Δ (see Equation (5)). Figures 1, 3, and 5 present the values of the parameter Δ as a measure of intermittency computed for fast (left column) and slow (right column) solar wind and the three magnetic field components B_R, B_T, and B_N. We also indicate the accuracy of the calculation of the parameter Δ. For comparison, in Figures 2, 4, and 6, we present the results of multifractal analysis preformed for magnetic field components transformed to the MF reference system: $B_\parallel$ (parallel to the mean field vector $\boldsymbol{B}_0$, panels (a) and (b)), and the two perpendicular components $B_{\perp 1}$ (panels (c) and (d)), $B_{\perp 2}$ (panels (e) and (f)). In the next subsections we discuss the radial and latitudinal dependences of multifractality as a measure of intermittency.

4.1. Variation of Inertial Range Intermittency with Radial Distance

Figures 1 and 2 show the variation of parameter Δ with the radial distance D, between 1.4 and 5.4 au from the Sun, in the fast and slow solar wind. The radial (Figure 1(a)), transversal (Figure 1(c)), and normal (Figure 1(e)) magnetic field components in the fast solar wind show a small decrease of intermittency with the distance from the Sun. The decreasing rate, determined by the least squares linear fit to the log–log
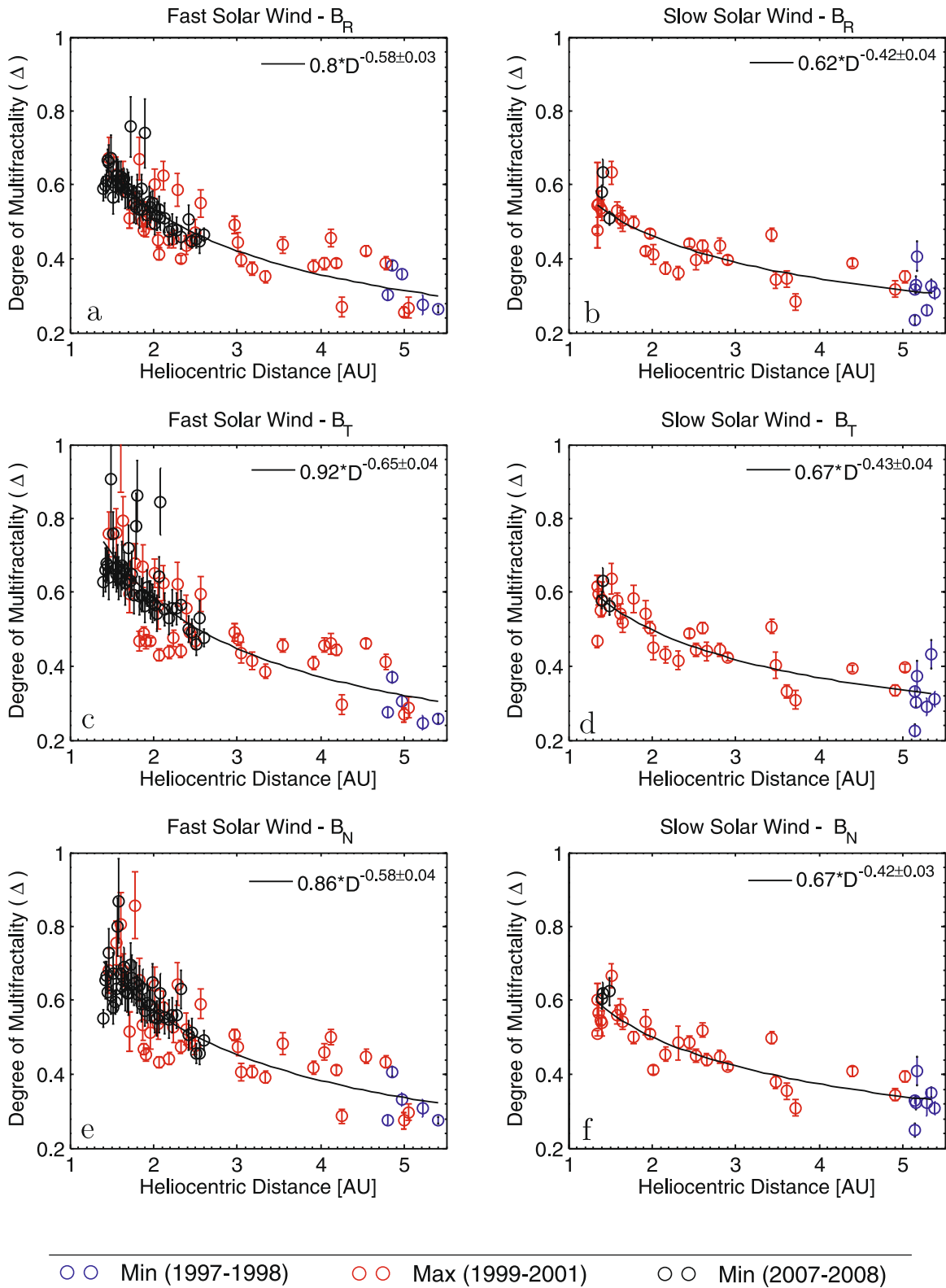
Figure 1. Degree of multifractality Δ as a measure of intermittency in radial B_R (panels (a) and (b)), transversal B_T (panels (c) and (d)), and normal B_N (panels (e) and (f)) magnetic field components as a function of the distance from the Sun. Data were collected during two solar minima (1997–1998, blue circles) and (2007–2008, black circles), and one solar maximum (1999–2001, red circles). Power-law fit $\Delta = aD^b$ to data is presented by a continuous line.

values of Δ against distance $D(\Delta = aD^b)$, differ between components. More precisely, for B_R and B_N we found $b = 0.58 \pm 0.03$ while for B_T the rate is slightly higher, $b = 0.65 \pm 0.03$. However, at heliocentric distances smaller than 2.5 au

we observe that the trend of variation departs slightly from this power-law regime. The analysis of data transformed to MF reference system (Figure 2) reveals similar behavior as that found for the RTN reference system. Again we
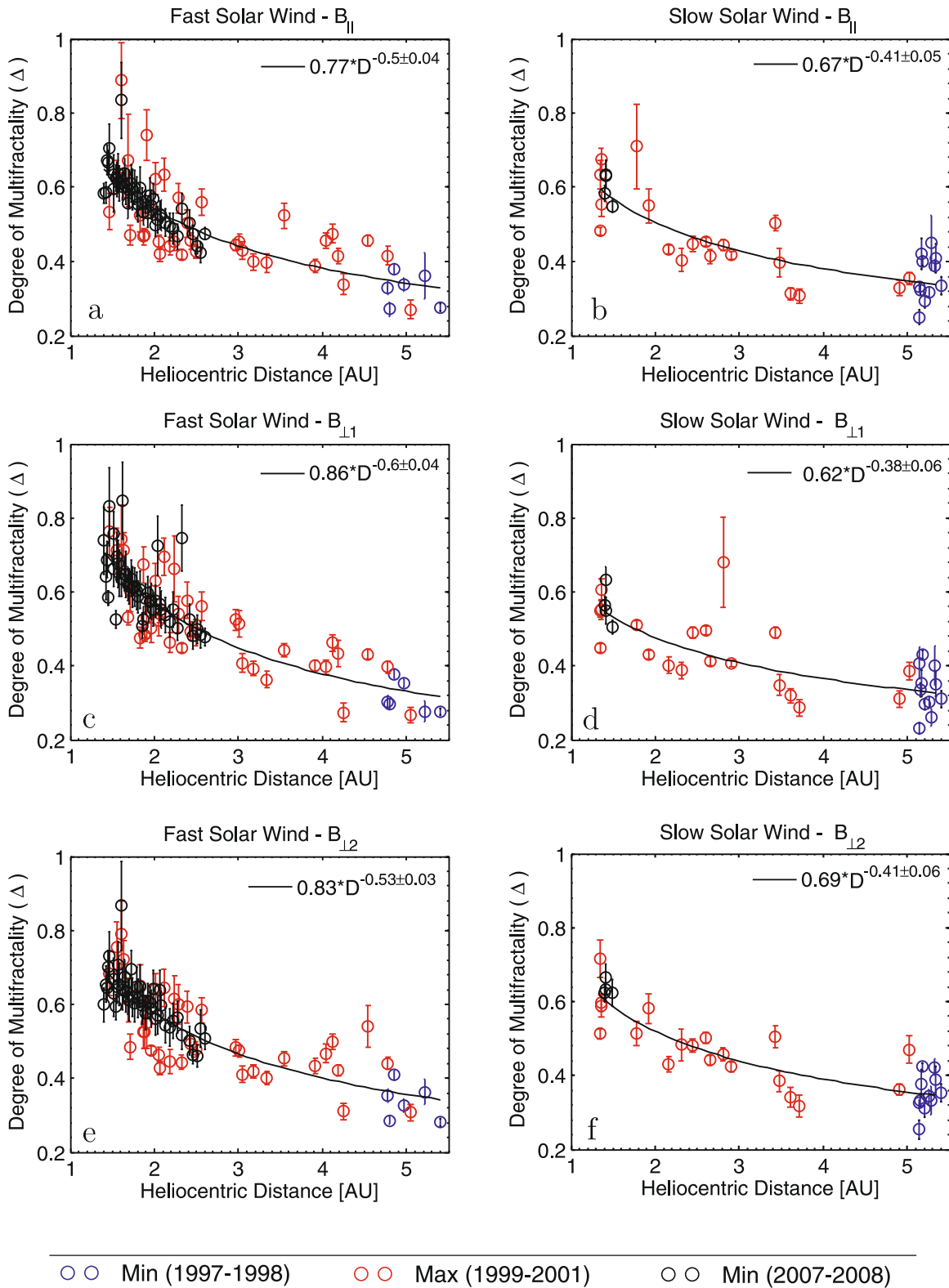
Figure 2. Degree of multifractality Δ as a measure of intermittency in magnetic field components measured during solar minima (1997–1998, 2007–2008) and solar maximum (1999–2001) and transformed to the MF reference system: $B_{\parallel}$ (parallel to the mean field vector $\boldsymbol{B}_0$, panels (a) and (b)), and two components $B_{\perp 1}$ (panels (c) and (d)) and $B_{\perp 2}$ (panels (e) and (f)), perpendicular to the field. Values of Δ presented as a function of the distance from the Sun together with the power-law fit $\Delta = aD^b$ to data marked by a continuous line.

observe the decrease of Δ with distance from the Sun, both for the parallel ($B_{\parallel}$) and perpendicular ($B_{\perp 1}$ and $B_{\perp 2}$) components. The smallest rate was found for $B_{\parallel}$, for which we have $b = 0.5 \pm 0.04$. For perpendicular components the parameter b varies from 0.53 ± 0.03 (for $B_{\perp 2}$) to 0.6 ± 0.04 (for $B_{\perp 1}$).

The results for the slow solar wind shown in Figures 1 and 2 (panels (b), (d), and (f)) are more difficult for the interpretation.

Table 2
The Variation Rate, b, of Multifractality (Intermittency) with the Radial Distance D ($\Delta = aD^b$) for the Fast and Slow Solar Wind Streams in RTN and MF Reference Systems

Scale	Fast Solar Wind		Slow Solar Wind	
	$\geqslant 16$ s	$\geqslant 2$ s	$\geqslant 16$ s	$\geqslant 2$ s
B_R	0.50 ± 0.03	0.39 ± 0.03	0.42 ± 0.04	0.20 ± 0.04
B_T	0.65 ± 0.04	0.39 ± 0.04	0.43 ± 0.04	0.27 ± 0.04
B_N	0.58 ± 0.04	0.37 ± 0.03	0.42 ± 0.03	0.32 ± 0.03
$B_\parallel$	0.50 ± 0.04	0.15 ± 0.06	0.41 ± 0.05	0.10 ± 0.05
$B_{\perp 1}$	0.60 ± 0.04	0.24 ± 0.05	0.38 ± 0.06	0.22 ± 0.06
$B_{\perp 2}$	0.53 ± 0.03	0.29 ± 0.04	0.41 ± 0.06	0.15 ± 0.07

Note. The table compares results from multifractal analysis at MHD scales ($\geqslant 16$ s) and kinetic scales ($\geqslant 2$ s).

We analyzed a smaller number of samples, most of them (marked by red circles), obtained from the maximum of solar cycle 23. Additionally, in a few cases the lack of a clear multifractal scaling did not allow us to determine the parameter Δ. Nevertheless, we can still observe a decrease of multifractality (intermittency) with radial distance but weaker than in the case of the fast solar wind. The parameter Δ for slow solar wind data in the RTN reference system decreases with distance D with rates of about 0.42 ± 0.03 (Figures 1(b), (d), and (f)). We obtained a similar behavior for components rotated into the MF reference system, as depicted in Figure 2(b), (d), and (f), with b in the range between 0.38 ± 0.06 (for component $B_{\perp 1}$) and 0.41 ± 0.05 (for $B_\parallel$ and $B_{\perp 1}$). The observed difference between components and reference systems seems to be rather negligible, particularly if we take into account the errors of the fit $\Delta = aD^b$, which are higher for the MF reference system.

Additionally, in order to compare with our previous analysis (Wawrzaszek et al. 2015), we performed a study, in which we included additional smaller scales, between 2 and 16 s. The rates obtained from power-law fit $\Delta = aD^b$ are summarized in Table 2 and compared to the ones corresponding to Figures 1 and 2.

Table 2 shows smaller values of b when scales smaller than 16 s are included in the multifractal analysis. Similar rate values (0.31 ± 0.03 for fast solar wind and 0.26 ± 0.04 for slow solar wind) have been found for multifractal analysis of magnetic field intensity (Wawrzaszek et al. 2015, Figure 2). This slower decrease of multifractality (intermittency) with distance can be somehow related to the higher level of intermittency at smaller scales, as confirmed by various studies (e.g., Marsch & Liu 1993; Sorriso-Valvo et al. 1999; Bruno et al. 2003; Alexandrova et al. 2008). Another interesting finding is that the intermittency of the parallel component $B_\parallel$ shows a negligible variation with distance, both in the fast and slow solar wind. We suggest that it can be due to the fact that compressive phenomena, more important in $B_\parallel$ (Bruno et al. 2003), start to be more active on scales smaller than 16 s. Alexandrova et al. (2008) showed that intermittency increases at kinetic scales possibly due to compressive effects.

On the basis of these results, we can tentatively conclude that the analysis of *Ulysses* data, mainly from the solar cycle 23, reveals a decrease of intermittency with increasing distance from the Sun. However, the rate of variation, is always higher for fast than for slow solar wind and presents significant anisotropy between the three components of the magnetic field.

The analysis shows that the smallest scales have a crucial role in determining the rate of radial variation of intermittency.

4.2. Latitudinal Variation of Inertial Range Intermittency

The latitudinal dependence of the degree of multifractality Δ as a measure of intermittency for the fast and slow solar wind cases are depicted in Figures 3 (multifractality of RTN components) and 4 (multifractality of MF components). For all cases of fast solar wind at solar minimum, we see a decrease of parameter Δ with the latitude increases; the smallest values are observed at solar poles. The symmetry with respect to the ecliptic plane is observed mainly for the fast solar wind, for all magnetic field components measured during solar minima (1997–1998, 2007–2008). This result confirms previous observations (Bavassano et al. 2000; Wawrzaszek & Macek 2010; Wawrzaszek et al. 2015) suggesting similar turbulent properties of the fast polar solar wind in the two hemispheres. On the other hand, we do not have a similar latitudinal dependence and symmetry during the solar maximum (1999–2001), for slow and fast solar wind. The more scattered behavior is observed, as the confirmation of the complex nature of the solar wind during the phase of the strong activity of the Sun.

Let us now discuss the results obtained for the solar minimum (1997–1998), at heliocentric distance (~5 au) and heliographic latitudes smaller than $20°$. For these data, we observe that the level of multifractality (intermittency) is lower for fast solar wind than for the slow wind which is in agreement with previous studies performed in the ecliptic (Marsch & Liu 1993; Bruno et al. 2003), and analysis of *Ulysses* data for the years 1992–1997 (Yordanova et al. 2009). However, data from solar maximum (1999–2001) and minimum (2007–2008) reveals cases when slow solar wind shows a lower level of multifractality (intermittency) than the fast solar wind. It is worth recalling that a similar conclusion has been given by Pagel & Balogh (2002), from data from the same solar maximum. This is a rather unexpected observation because the fast solar wind is more Alfvénic than slow solar wind. The main contribution to solar wind intermittency is due to non-Alfvénic structures, while Alfvénic increments are found to be characterized by a smaller level of intermittency than the previous ones (e.g., D'Amicis et al. 2012). To better understand these results we note that most of the slow solar wind cases considered in our analysis pertain to solar cycle 23, which had quite peculiar properties (e.g., McComas et al. 2008; D'Amicis et al. 2011). In particular, the maximum of solar cycle 23 (the year 2001) was largely dominated by slow wind as expected, which, however, showed a high degree of Alfvénicity comparable or even higher than that found in the fast wind during the minimum of the same cycle (2007) as discussed by D'Amicis et al. (2011). Moreover, recent studies suggest the existence of a new type of Alvénic slow wind having some characteristics common to the fast wind (D'Amicis & Bruno 2015). Perhaps, our analysis can be seen as an independent confirmation of these suggestions.

Furthermore, analysis of results presented in Figures 3 and 4 reveals some differences between magnetic field components. In general, in Figures 3(a), (c), and (e), which correspond to fast solar wind data, we observe higher levels of intermittency for the transversal B_T and normal B_N components, for which most of the values of parameter Δ are in the range of about 0.4–0.8, while in the case of B_R most results present a level of multifractality Δ below 0.6. This observation confirms previous analyses beyond the ecliptic (Pagel & Balogh 2001, 2003; Nicol et al. 2008). Differences between multifractality (intermittency) of magnetic
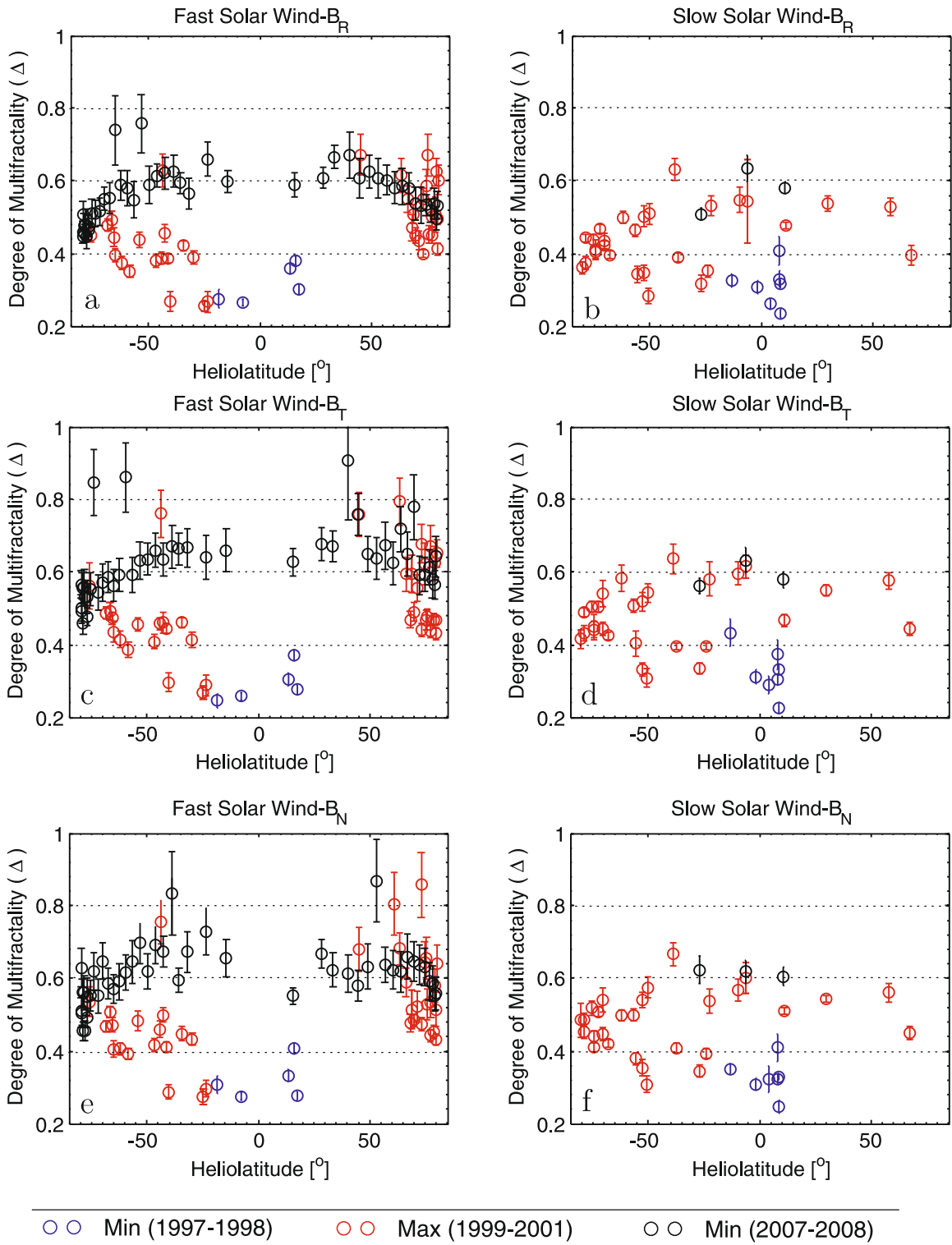
Figure 3. Parameter Δ quantifying multifractality (intermittency) in the magnetic field components B_R (a), (b), B_T (c), (d), B_N (e), (f) measured in RTN reference system as a function of the heliographic latitude during solar minima (1997–1998, 2007–2008) and solar maximum (1999–2001), respectively.

components in the case of the slow solar wind (Figures 3(b), (d), and (f)) are rather negligible, with the values of parameter Δ smaller than 0.6, in general. Results for data transformed to the MF reference system, as shown in Figure 4, also reveal differences between components $B_{\parallel}$ (panel (a)), $B_{\perp 1}$ (panels (c)), and $B_{\perp 2}$ (panel (e)). The slightly higher level of intermittency is observed for perpendicular components, which also present

some differences between each other, especially for positive latitudes. The lack of the expected significant differences between these components, in particular, the more intermittent state of the $B_{\parallel}$, as shown by Bruno et al. (2003), can be connected with rather weak contributions of compressive effects on the turbulent behavior. This effect seems to be stronger on smaller scales as we have shown in the previous subsection.
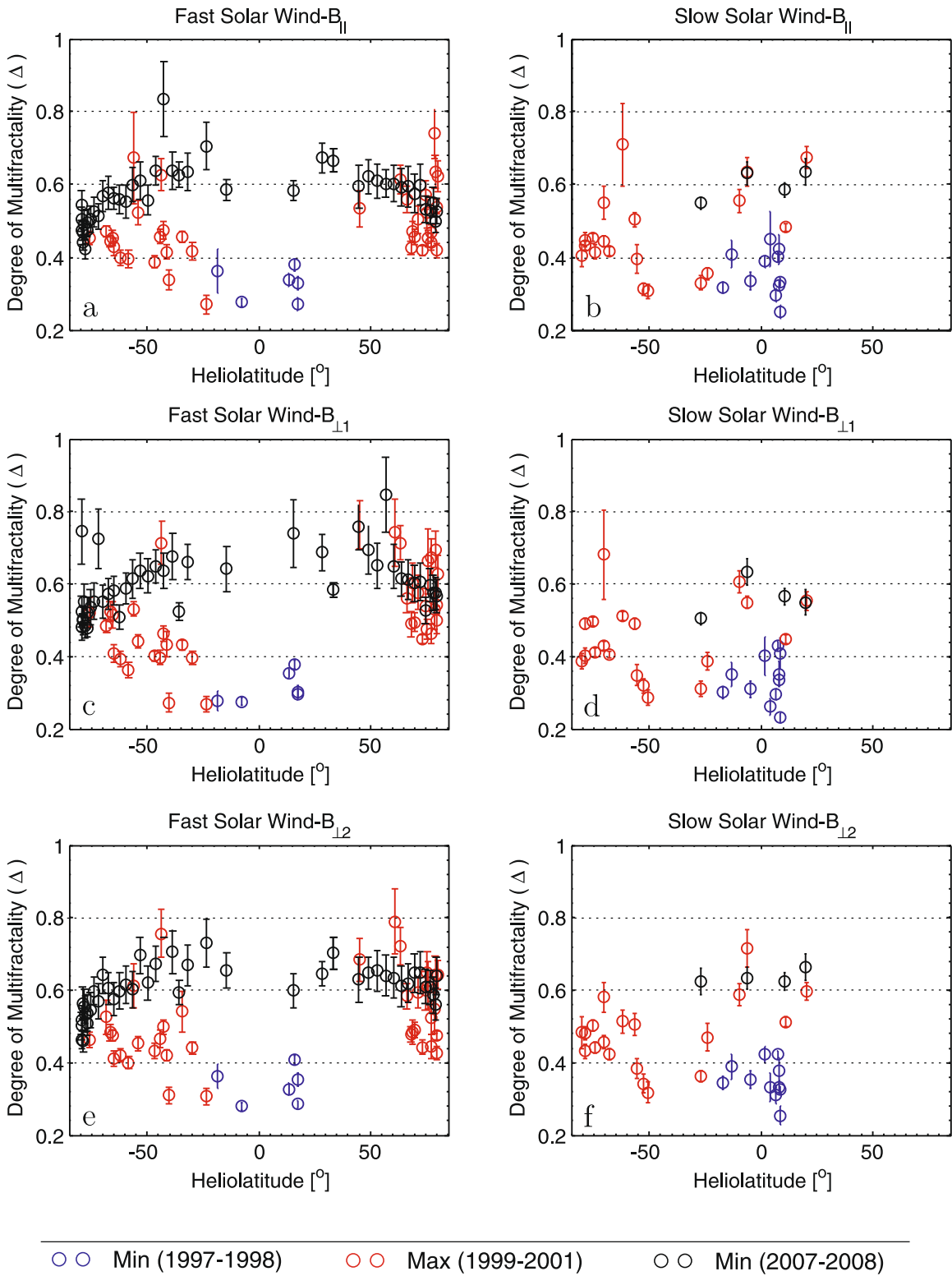
Figure 4. Latitudinal dependence of the parameter Δ, quantifying multifractality (intermittency) in magnetic field components measured during solar minima (1997–1998, 2007–2008) and solar maximum (1999–2001). Data were transformed to the MF reference system: $B_\parallel$ (parallel to the mean field vector $\boldsymbol{B}_0$, panels (a) and (b)), and two components $B_{\perp 1}$ (panels (c) and (d)), $B_{\perp 2}$ (panels (e) and (f)), perpendicular to the field, respectively.

4.3. Maps of Multifractality (Intermittency)

In view of the results of the previous subsections, especially for the second minimum (2007–2008), marked in Figures 1–4 by black circles, we see that the effect of change of solar wind multifractality with heliographic latitude may partially interfere with the variation of this parameter with distance from the Sun. However, it is difficult to separate the latitudinal and radial evolution of intermittency in *Ulysses* data. Therefore, we choose to represent the level of multifractality as a function of
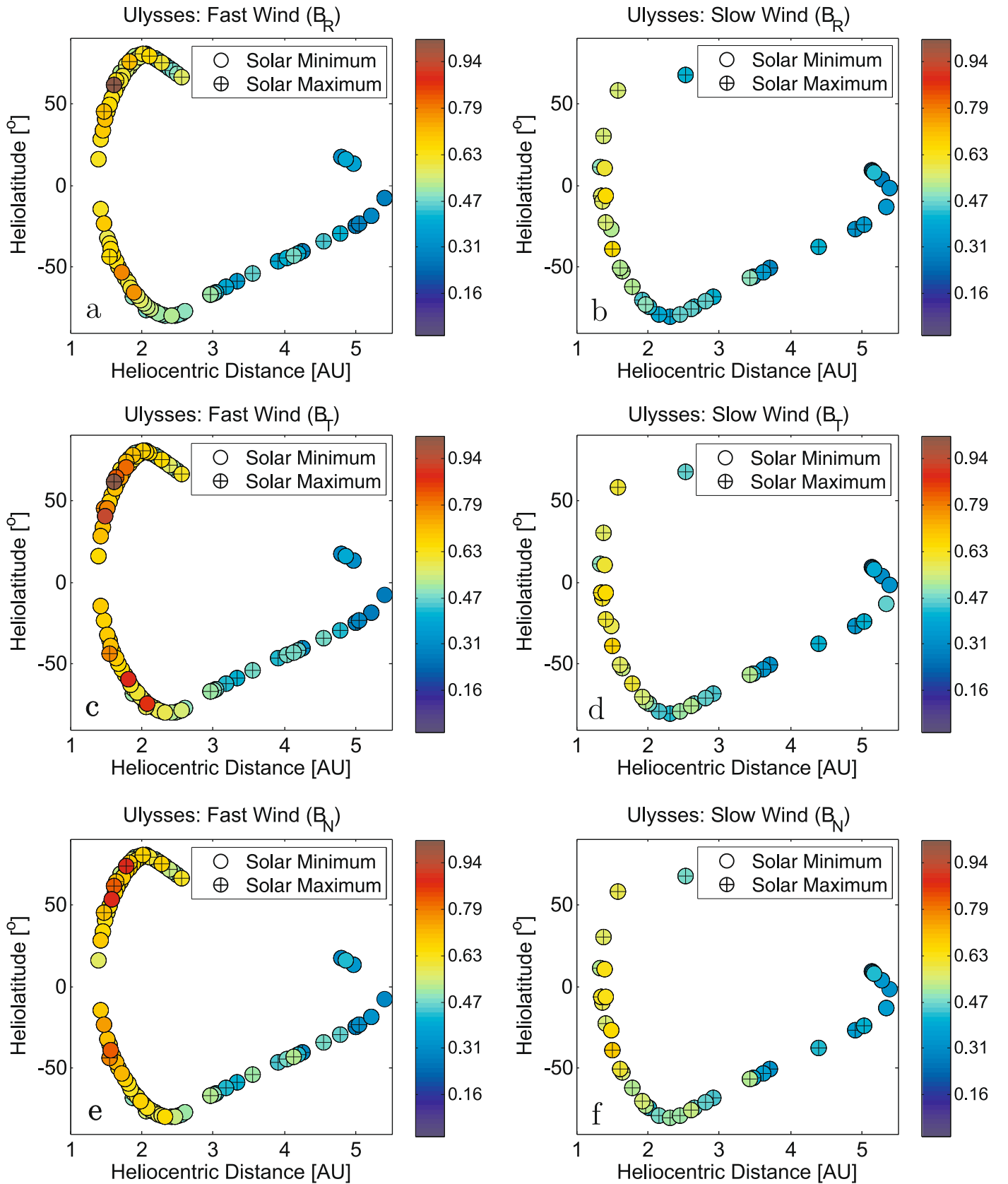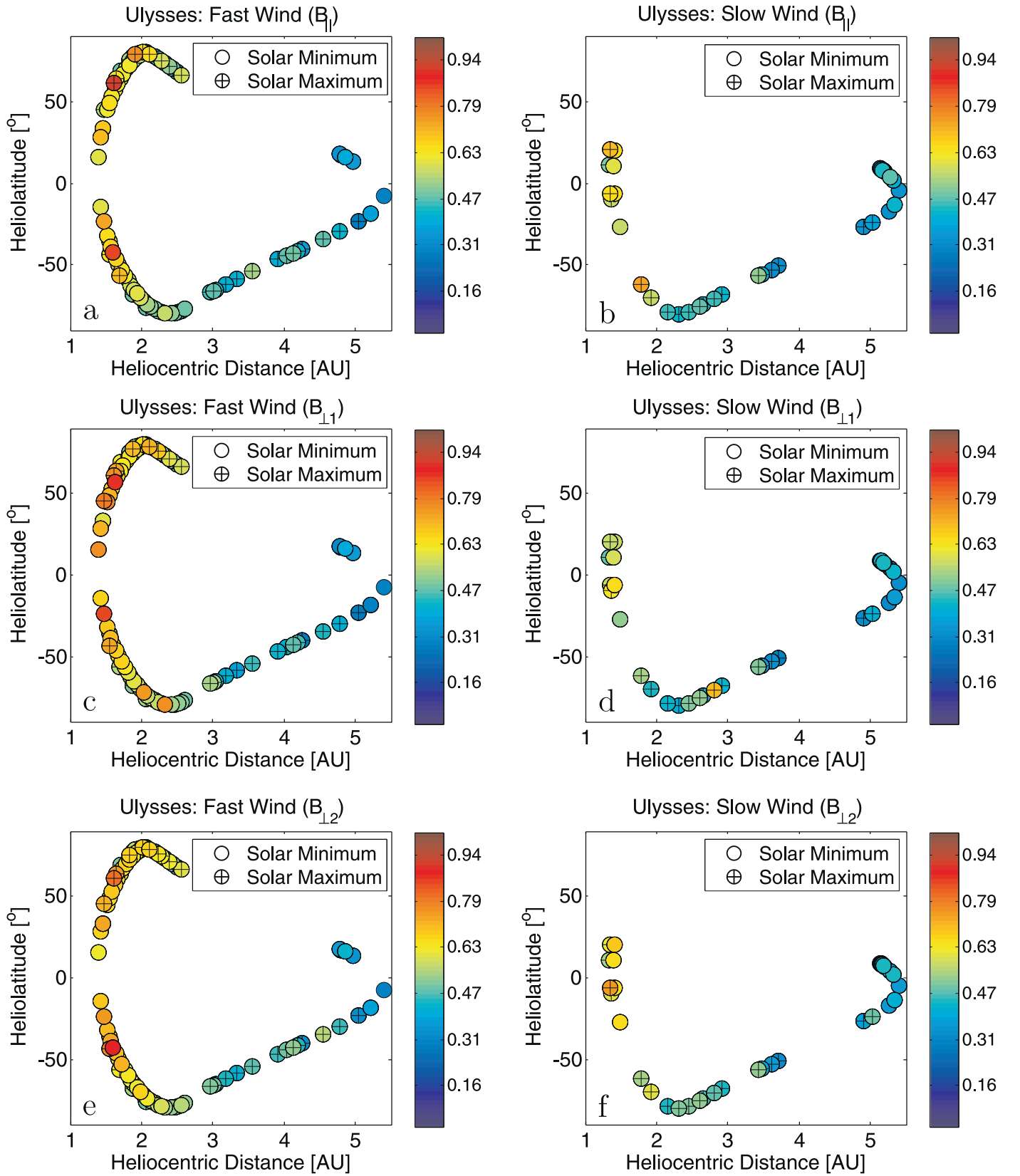
Figure 5. Maps of the degree of multifractality as a measure of intermittency determined for fast (left panel) and slow (right panel) solar wind system during solar minima (1997–1998, 2007–2008) and solar maximum (1999–2001), respectively. Color denotes the values of the parameter Δ determined for three magnetic field components: B_R (a), (b), B_T (c), (d), B_N (e), (f) in RTN reference system at different heliocentric distances and heliographic latitudes.

Figure 6. Maps of the degree of multifractality as a measure of intermittency determined for the fast (left panel) and slow (right panel) solar wind system during solar minima (1997–1998, 2007–2008) and solar maximum (1999–2001), respectively. Color denotes the values of the parameter Δ determined for the components $B_{\parallel}$ (parallel to the mean field vector $\boldsymbol{B}_0$, panels (a) and (b)), and two components perpendicular to the field: (1) $B_{\perp 1}$ (panels (c) and (d)), $B_{\perp 2}$ (panels (e) and (f)), as observed by *Ulysses* at different heliocentric distances and heliographic latitudes.

both heliocentric distance and heliographic latitude. Figures 5 and 6 show maps of multifractality along *Ulysses*' orbit, where color denotes the values of the parameter Δ determined for magnetic field fluctuation in RTN and MF reference systems, respectively. The maps clearly show that the fluctuations of the magnetic field in the fast solar wind are most intermittent at small distances from the Sun and this observation is generally independent of the considered magnetic field component. In the case of the slow solar wind, this effect is less significant, differences between components are less obvious. Our analysis shows that the intermittency depends more strongly on the structure of the solar wind than the phase of the solar cycle (Pagel & Balogh 2002). Moreover, the analysis of *Ulysses*' magnetic field data suggests a somewhat smaller degree of multifractality, $\Delta < 1.0$ than obtained previously for velocity fluctuations, $\Delta = 1.34$–1.52 (Wawrzaszek & Macek 2010).

5. Discussions and Conclusions

In this paper, we have studied the scaling properties of high-resolution *Ulysses* magnetic field fluctuations, measured beyond the ecliptic plane at a wide range of heliocentric distances between 1.4 and 5.4 au, at heliolatitudes from 80°S to 80°N. In order to avoid mixing of different physical conditions, we performed a systematic selection of a large number of cases of fast and slow solar wind during two solar minima (1997–1998, 2007–2008) and one solar maximum (1999–2001). The analysis provided about 750 multifractal spectra that helped to describe the intermittency in the MHD regime (at scales larger than 16 s) for all magnetic field components in two reference systems: RTN and MF. The main findings of this work can be summarized as follows.

Previous analysis of intermittency in the ecliptic showed the increase with radial distance. Our study points toward a slow decrease of degree of multifractality as a measure of intermittency with distance and with latitude, as initially suggested in a previous analysis of magnetic field intensity (Wawrzaszek et al. 2015). This behavior is observed in all magnetic field components, regardless of the reference system used (RTN or MF). The higher rate of intermittency decrease has been found for the fast solar wind, for transversal components in RTN and perpendicular components in the MF reference system. The smallest scales significantly influence the values of the variation rates. In general our analysis seems to support the idea that the intermittency in MHD range has a solar origin (Pagel & Balogh 2002; Wawrzaszek et al. 2015), while the reduced efficiency of drivers (fast and slow streams, shocks interaction, pressure balanced, almost incompressible current sheets, and interplanetary shocks as suggested by Veltri & Mangeney 1999) does not maintain the level of intermittency with the distance from the Sun. Additionally, analysis of intermittency over a large range of heliographic latitudes confirmed similar intermittent properties of the fast solar wind turbulence observed in the two hemispheres, as reported in previous studies (Bavassano et al. 2000; Wawrzaszek & Macek 2010; Wawrzaszek et al. 2015).

The comparison of the slow solar wind intermittency measured during the solar minimum (1997–1998) at distances ~5 au and close to the equatorial plane presents a higher level of intermittency than the fast solar wind. This confirms previous results (e.g., Bruno et al. 2003; Yordanova et al. 2009) and the need for the separate analysis of the two types of wind. However, analysis of the slow solar wind from solar maximum (1999–2001)

and from the second solar minimum (2007–2008) showed in many cases a smaller level of intermittency than for the fast solar wind. The observation of a high degree of Alfvénicity for slow solar wind during solar maximum (2001), as found by D'Amicis et al. (2011), seems to explain this unusual behavior, as well as the much higher level of multifractality (intermittency) in data from the solar minimum (2007–2008). However, only a detailed analysis of Alfvénicity, as well as the further improvement of the data selection procedure by considering additional parameters (see, e.g., Landi et al. 2012; Xu & Borovsky 2015), especially in the context of classification of the slow solar wind in more than two categories (D'Amicis & Bruno 2015), will allow a more detailed verification of this hypothesis.

Our study suggests that transverse components exhibit a slightly higher level of intermittency than the radial component, similarly to other studies devoted to turbulence beyond the ecliptic (e.g., Pagel & Balogh 2001, 2003). We noticed relatively small differences between intermittency of parallel and perpendicular components. This difference increased when scales less than 16 s were included in the analysis, possibly due to increased intermittency at kinetic scales. Bruno et al. (1999) proved that the observed level of magnetic anisotropy strongly depends on intermittency. Our analysis seems to confirm this fact. In particular, the highest level of anisotropy is observed close to the Sun, where intermittency is the strongest. However, because we do not find an increase of intermittency with the radial distance, we do not observe an increase of differences between magnetic field components, contrary to what was found in the ecliptic from *Helios* data (e.g., Bruno et al. 1999, 2003).

Finally, Sorriso-Valvo et al. (2017) pointed out that different measures of intermittency capture different aspects of fluctuation topology. The multifractal description of the solar wind intermittency based on PF function provides an important complement to previous analyses. In particular, multifractal analysis considers higher-order moments magnifying large or small concentrations of measure, while in the case of basic methods devoted to intermittency only positive or particular moments are used. Therefore, the multifractal spectrum and the degree of multifractality determined in this paper at small scales, provide a complete quantitative and qualitative description of the structure of intermittent magnetic field fluctuations. Nevertheless, we are convinced that the statistical description, in particular, the fourth moment of PDF, can still provide an appropriate complementary tool to help us understand the still puzzling aspects of intermittent turbulence beyond the ecliptic.

In summary, the comparison of the intermittent signatures of the magnetic field fluctuations at two very different levels of solar activity over a large range of heliographic latitudes confirms the nonuniversal and complex nature of solar wind turbulence, and underline the importance of selecting homogeneous samples when performing the analysis.

ORCID iDs

Anna Wawrzaszek ● https://orcid.org/0000-0001-9946-3547
Marius Echim ● https://orcid.org/0000-0001-7038-9494
Roberto Bruno ● https://orcid.org/0000-0002-2152-0115

References

Alexandrova, O., Carbone, V., Veltri, P., & Sorriso-Valvo, L. 2008, ApJ, 674, 1153
Balogh, A., Beek, T. J., Forsyth, R. J., et al. 1992, A&AS, 92, 221
Bame, S. J., McComas, D. J., Barraclough, B. L., et al. 1992, A&AS, 92, 237
Bavassano, B., Pietropaolo, E., & Bruno, R. 2000, JGR, 105, 15959
Bavassano, B., Pietropaolo, E., & Bruno, R. 2001, JGRA, 106, 10659
Bruno, R., & Bavassano, B. 1991, JGRA, 96, 7841
Bruno, R., Bavassano, B., Pietropaolo, E., Carbone, V., & Veltri, P. 1999, GeoRL, 26, 3185
Bruno, R., & Carbone, V. 2013, LRSP, 10, 2
Bruno, R., Carbone, V., Sorriso-Valvo, L., & Bavassano, B. 2003, JGRA, 108, 1130
Bruno, R., Carbone, V., Veltri, P., Pietropaolo, E., & Bavassano, B. 2001, P&SS, 49, 1201
Bruno, R., & Trenchi, L. 2014, ApJL, 787, L24
Bruno, R., Trenchi, L., & Telloni, D. 2014, ApJL, 793, L15
Burlaga, L. 1995, Interplanetary Mganetohydrodynamics (1st ed.; New York: Oxford Univ. Press)
Burlaga, L. F. 1991a, JGRA, 96, 5847
Burlaga, L. F. 1991b, GeoRL, 18, 69
Burlaga, L. F., & Ness, N. F. 2010, ApJ, 725, 1306
Burlaga, L. F., Perko, J., & Pirraglia, J. 1993, ApJ, 407, 347
Castaing, B., Gagne, Y., & Hopfinger, E. 1990, PhyD, 46, 177
Chhabra, A., & Jensen, R. V. 1989, PhRvL, 62, 1327
D'Amicis, R., & Bruno, R. 2015, ApJ, 805, 84
D'Amicis, R., Bruno, R., & Bavassano, B. 2011, JASTP, 73, 653
D'Amicis, R., Consolini, G., Bavassano, B., & Bruno, R. 2012, ApJ, 755, 63
Falconer, K. 1990, Fractal Geometry: Mathematical Foundations and Applications (1st ed.; New York: Wiley)
Farge, M. 1992, AnRFM, 24, 395
Frisch, U. 1995, Turbulence. The Legacy of A.N. Kolmogorov (Cambridge: Cambridge Univ. Press)
Gloeckler, G., Geiss, J., Balsiger, H., et al. 1992, A&AS, 92, 267
Grassberger, P., & Procaccia, I. 1983, PhRvL, 50, 346
Halsey, T. C., Jensen, M. H., Kadanoff, L. P., Procaccia, I., & Shraiman, B. I. 1986, PhRvA, 33, 1141
Horbury, T., Balogh, A., Forsyth, R., & Smith, E. 1997, AdSpR, 19, 847
Horbury, T. S., & Balogh, A. 2001, JGRA, 106, 15929
Horbury, T. S., Balogh, A., Forsyth, R. J., & Smith, E. J. 1996, A&A, 316, 333
Howes, G. G., Klein, K. G., & TenBarge, J. M. 2014, ApJ, 789, 106
Kantelhardt, J. W., Zschiegner, S. A., Koscielny-Bunde, E., et al. 2002, PhyA, 316, 87
Kasper, J. C., Stevens, M. L., Korreck, K. E., et al. 2012, ApJ, 745, 162
Lamy, H., Wawrzaszek, A., Macek, W. M., & Chang, T. 2010, in AIP Conf. Proc. 1216, Twelth International Solar Wind Conf. (Melville, NY: AIP), 124
Landi, E., Alexander, R. L., Gruesbeck, J. R., et al. 2012, ApJ, 744, 100
Lepri, S. T., Landi, E., & Zurbuchen, T. H. 2013, ApJ, 768, 94
Macek, W. M., & Szczepaniak, A. 2008, GeoRL, 35, L02108
Macek, W. M., & Wawrzaszek, A. 2009, JGRA, 114, A03108
Macek, W. M., Wawrzaszek, A., & Burlaga, L. F. 2014, ApJL, 793, L30
Macek, W. M., Wawrzaszek, A., & Carbone, V. 2011, GeoRL, 38, L19103
Mandelbrot, B. B. 1989, PApGe, 131, 5
Marsch, E., & Liu, S. 1993, AnGeo, 11, 227
Marsch, E., & Tu, C. Y. 1994, AnGeo, 12, 1127
Marsch, E., Tu, C.-Y., & Rosenbauer, H. 1996, AnGeo, 14, 259
McComas, D. J., Ebert, R. W., Elliott, H. A., et al. 2008, GeoRL, 35, L18103
Meneveau, C., & Sreenivasan, K. R. 1987, PhRvL, 59, 1424
Nicol, R. M., Chapman, S. C., & Dendy, R. O. 2008, ApJ, 679, 862
Ott, E. 1993, Chaos in Dynamical Systems (1st ed.; Cambridge: Cambridge Univ. Press)
Pagel, C., & Balogh, A. 2001, NPGeo, 8, 313
Pagel, C., & Balogh, A. 2002, JGRA, 107, SSH6
Pagel, C., & Balogh, A. 2003, JGRA, 108, SSH2
Perri, S., Goldstein, M. L., Dorelli, J. C., & Sahraoui, F. 2012, PhRvL, 109, 191101
Perri, S., Servidio, S., Vaivads, A., & Valentini, F. 2017, ApJS, 231, 4
Ruzmaikin, A. A., Feynman, J., Goldstein, B. E., Smith, E. J., & Balogh, A. 1995, JGR, 100, 3395
Saucier, A., & Muller, J. 1999, PhyA, 267, 221
Sorriso-Valvo, L., Carbone, F., Leonardis, E., et al. 2017, AdSpR, 59, 1642
Sorriso-Valvo, L., Carbone, V., Giuliani, P., et al. 2001, P&SS, 49, 1193
Sorriso-Valvo, L., Carbone, V., Veltri, P., Consolini, G., & Bruno, R. 1999, GeoRL, 26, 1801
Szczepaniak, A., & Macek, W. M. 2008, NPGeo, 15, 615
Taylor, G. I. 1938, RSPSA, 164, 476
Tu, C.-Y., Marsch, E., & Rosenbauer, H. 1996, AnGeo, 14, 270
Veltri, P., & Mangeney, A. 1999, in AIP Conf. Ser. 471, ed. S. R. Habbal et al., 543
Wan, M., Matthaeus, W. H., Karimabadi, H., et al. 2012, PhRvL, 109, 195001
Wawrzaszek, A., Echim, M., Macek, W. M., & Bruno, R. 2015, ApJL, 814, L19
Wawrzaszek, A., & Macek, W. M. 2010, JGRA, 115, A07104
Xu, F., & Borovsky, J. E. 2015, JGRA, 120, 70
Yordanova, E., Balogh, A., Noullez, A., & von Steiger, R. 2009, JGRA, 114, A08101
Zurbuchen, T. H., Fisk, L. A., Gloeckler, G., & von Steiger, R. 2002, GeoRL, 29, 66